Theor Chem Acc (2000) 103:380–389
DOI 10.1007/s002149900066

Theoretical
Chemistry Accounts


*Regular article*

# Conformational profile of 1-aminocyclopropanecarboxylic acid

**Jesus Gomez-Catalan[1], Carlos Aleman[2], Juan J. Perez[2]**

[1] Unitat de Toxicologia, Facultat de Farmacia, Universitat de Barcelona, Av. Joan XXIII s/n, E-08028 Barcelona, Spain
[2] Departamento d'Enginyeria Quimica, UPC, ETS d'Enginyeria, Av. Diagonal 647, E-08028 Barcelona, Spain

Received: 19 March 1999 / Accepted: 10 June 1999 / Published online: 9 September 1999

**Abstract.** 1-Aminocyclopropanecarboxylic acid ($Ac_3c$) is a constrained $\alpha$ amino acid residue that exhibits peculiar conformational characteristics. The aim of the present study is to provide a deeper understanding of these features to be used as guidance to decide when to choose $Ac_3c$ as a building block for the design of peptide and protein surrogates. The whole Ramachandran plot of the Ace-$Ac_3c$-$NCH_3$ dipeptide was investigated at the Hartree–Fock level using a 6-31G(d) basis set and the most favorable structures were assessed on this surface by energy minimization. These results were subsequently used as a reference to generate specific molecular mechanics parameters for $Ac_3c$ compatible with the parm94 set of the AMBER force field. The effect of water as a solvent on the conformational profile of the dipeptide was also assessed using the Miertus–Scrocco–Tomasi self-consistent reaction-field model at the Hartree–Fock level using a 6-31G(d) basis set and using the AM1 semiempirical method. The conformational profile of the $Ac_3c$ dipeptide can be characterized by two symmetric low-energy regions for values of $\phi$ around $\pm 80°$ with a wide range of values for $\psi$ ranging from $-40$ to 180°, with the lower areas located at low values of $\psi$. Solvent effects do not alter the features of the conformational map, but a shift of the two absolute minima to ($\phi$, $\psi$) values near ($\pm 90°$, 0°) can be observed. These results are in accord with all experimental evidence and with the known tendency of $Ac_3c$ to induce $\beta$-turn conformations in peptides.

**Key words:** Constrained amino acids – Cyclopropane amino acids – Conformational study – Solvent effects on conformation

## 1 Introduction

Knowledge of the conformation that a peptide exhibits when bound to its receptor represents key information for the design of peptide surrogates and peptidomimetics [1, 2]. An indirect approach widely used in the past to assess the features of the bioactive form of a peptide was the synthesis of peptide analogs with restricted conformational freedom. There is extensive literature covering successful achievements obtained in the past using this approach [3–5]. Constraints imposed on the analogs can be global by cyclization of the peptide, or local by incorporating conformationally constrained amino acid residues into the peptide sequence; however, for efficient use of the latter approach a profound knowledge of the conformational features of the building blocks incorporated into the sequence is necessary. Computational methods can provide useful insights in this field.

The accessible conformational space of an amino acid residue can essentially be characterized by its potential-energy map, generated from systematic rotation of the backbone dihedral angles $\phi$ and $\psi$ defined by the $N{-}C^{\alpha}$ and $C^{\alpha}{-}C$ bonds, respectively. Most of the natural amino acid residues can access about 30% of the ($\phi$, $\psi$) space. Glycine is the most flexible amino acid residue, accessing more than 60% of the conformational space [6]. In contrast, proline is the only natural amino acid residue with its accessible conformational space considerably reduced [7], a feature adequately exploited to generate inverse turns in peptide sequences [8]. Unnatural, conformationally restricted amino acid residues expand the repertoire of available building blocks to control peptide secondary structure [9, 10]. There are several strategies to constrain amino acid residues to reduce their energy-accessible conformational space. Among them, substitution of the $\alpha$-carbon hydrogen to restrict both backbone and side-chain conformational freedom has been widely investigated [11, 12].

1-Aminocyclopropanecarboxylic acid ($Ac_3c$) belongs to the family of 1-aminocycloalkanecarboxylic acids, exhibiting a restricted conformational space. Crystallographic studies carried out on different di- or tripeptide analogs containing this $\alpha$,$\alpha$-dialkylated residue have revealed well-defined conformational preferences [13–15]. Specifically, values of $+80$ and $-80°$ with similar propensity have been found for the angle $\phi$, whereas $\psi$ adopts values of either 0 or 180°, with the former

*Correspondence to*: J.J. Perez

ocurring more often. Similar behavior has also been observed in cyclopropane derivatives with a carbonyl group, where the plane defined by the carbonyl bond and its adjacent bond in all the structures bisects the ring [16]. This peculiar conformational behavior provides this residue with unique structural features that can be exploited for peptide surrogate design.

Quantum mechanics calculations performed at different theoretical levels have provided some understanding of the peculiar conformational behavior of $Ac_3c$. In a comparative study, Barone et al. [17] carried out ab initio calculations at the Hartree–Fock (HF) level using a STO-3G basis set to map the conformational space of the amino acid residue. In a more recent study, one of us [18] reported the energy minima of the $Ac_3c$ dipeptide at the HF level using both 3-21G and 6-31G(d) basis sets as well as at the MP2 level using the latter basis set. These studies suggest that calculations carried out with small basis sets provide a spurious minimum and an incorrect energy order of the minima.

With regard to molecular mechanics calculations, Barone et al. [17] and Taylor et al. [19] pointed out that standard force-field parameters cannot properly account for the conformational preferences of $Ac_3c$. Specifically, standard force fields display three important deficiencies:

1. Stretching and bending parameters do not reflect the strained nature of the three-membered ring, leading to erroneous equilibrium geometries.
2. The preferred conformations in the neighborhood of $\psi = 0°$ cannot be reproduced.
3. The stability of the conformations with $\psi = 180°$ is underestimated. In order to solve these difficulties an ad hoc incorporation of a twofold torsional potential with a barrier of 4.4 kcal/mol for $\psi$ was proposed to describe the conformational features of cyclopropane derivatives [17]. This barrier incorporated into the MM2 force field, provides conformations in agreement with experimental observations [17, 19]. With regard to the force constants and equilibrium parameters, we reported in a recent work a parametrization for the stretching and bending parameters of cyclopropane [20]. Such parameters provide molecular geometries in good agreement with experimental determinations and are also able to reproduce the frequencies of vibration of the cyclopropane ring; however as shown later, introduction of new torsional parameters is required in order to fit the specific characteristics of the ab initio $Ac_3c$ dipeptide conformational map.

In this work we have investigated the whole potential-energy surface of this amino acid residue using quantum mechanical calculations. The goal of the present study is

1. To extend the conformational studies previously reported, providing a whole description of $(\phi, \psi)$ space in vacuo, in order to know its features as well as the extension of the low-energy areas that constitute the accessible conformational space.
2. To investigate the effects induced by the aqueous solvent on such potential-energy surfaces using a self-consistent reaction-field (SCRF) method.
3. To provide a set of torsional parameters compatible with the AMBER force field to study the conformational profiles of peptides containing these residues in their sequence using molecular mechanics simulations.

Assessment of the quality of the new parameters developed was carried out by comparison of the Ramachandran plots obtained from empirical and quantum mechanical calculations.

## 2 Methods

### *2.1 Gas-phase calculations*

Ab initio calculations at the HF level using medium-size of basis sets have proven in the past to be very useful to describe the conformation features of amino acid residues [21–23]. Accordingly, calculations to map the Ramachandran plot of the $Ac_3c$ dipeptide were carried out at the HF/6-31G(d) level [24]. Calculations were performed on a grid of points on the $(\phi, \psi)$ space at 30° intervals. Due to the achiral nature of the molecule, only a half of the map was computed, since $E(\phi, \psi) = E(-\phi, -\psi)$. At each point of the grid the geometry was optimized by keeping the dihedral angles $\phi$ and $\psi$ constrained during the minimization process. Possible energy minima on the surface were investigated on every low-energy region of the map by full geometry optimizations. In order to evaluate the effect of electronic correlation, single-point MP2/6-31G(d) calculations without geometry optimization were carried for all the minima characterized and for two cross sections of the potential-energy surface.

### *2.2 Aqueous-phase calculations*

Solvent effects were computed within the Miertus–Scrocco–Tomasi (MST) SCRF model [25, 26]. Briefly, this method uses a quantum mechanical description of the solute and a "quasi" continuum representation of the solvent that is considered as a dielectric which reacts against the solute charge distribution, generating a reaction field. The effect of this reaction field is introduced by means of a perturbation operator ($V_R$) in the solute Hamiltonian (Eq. 1)

$$(H^0 + V_R)\psi = E\psi \ . \tag{1}$$

The MST method defines the perturbation operator in terms of the charge density induced by the solute charge distribution (derived from the fitting of the molecular electrostatic potential) in the solvent cavity surface. Imaginary charges are determined by solving the Laplace equation at the solute/solvent interface [27, 28]. The solvent cavity is built to fit the molecular geometry of the solute by applying a scaling factor of 1.25 to the van der Waals radii [28]. Solution of Eq. (1) leads to a new charge distribution, which in turn induces a new solvent charge distribution and the process is repeated until convergence.

The free energy of solvation ($\Delta G_{sol}$) is determined from the addition of an electrostatic (polarization) and a steric term, the latter being the sum of the cavitation and van der Waals contributions (Eq. 2)

$$\Delta G_{\mathrm{sol}} = \Delta G_{\mathrm{pol}} + \Delta G_{\mathrm{cav}} + \Delta G_{\mathrm{vdW}} \ . \tag{2}$$

The electrostatic free energy is computed according to Eq. (3), where the zero superscript stands for the gas phase, and the third term accounts for the work involved in the polarization of the solvent [25–27]

$$\Delta G_{\mathrm{pol}} = \langle\psi|H|\psi\rangle - \langle\psi^0|H|\psi^0\rangle - 1/2\left\{\langle\psi|V|\psi\rangle + \int \rho_{\mathrm{nuc}} V_\sigma(s)ds\right\} \ . \tag{3}$$

The cavitation term was determined using Pierotti's particle theory [29], while the van der Waals term was evaluated by means of a linear relation with the molecular surface area [27, 28] (Eq. 4).

$$\Delta G_{vdW} = \Sigma_i \xi_i S_i \quad , \tag{4}$$

where $S_i$ is the portion of the molecular surface area belonging to atom $i$ and $\xi_i$ is the van der Waals parameter of atom $i$.

The MST method accounts well for the solvent effects, its major limitation being the size of the system under consideration. For large systems, the MST model may be used satisfactorily within the semiempirical AM1 Hamiltonian framework [28]. In order to evaluate the differences between the two levels of computation for $Ac_3c$, solvent effects for the energy minima of the dipeptide were computed both at the ab initio level [restricted HF level with a 6-31(d) basis set] and with an AM1 framework. The good agreement observed between the results provided by two levels of approximation, permitted us to investigate the effect of the aqueous solvent on the whole potential-energy surface using the less demanding MST/AM1 method.

### 2.3 Force-field parameterization

Force-field parameters consistent with the Cornell (parm94) parameterization of the AMBER force field [29] were developed for the $Ac_3c$ amino acid residue. A new carbon atom type (C4) was defined for the cyclopropane carbons. Since cyclopropane bond-stretching and angle-bending force constants are not very sensitive to the level of the theory employed for their derivation [20], the AM1 semiempirical method [30] was chosen in the present work for their derivation. Bond-stretching and angle-bending parameters involving C4 atom types were directly derived on the $Ac_3c$ dipeptide using the program for approximate parametrization from quantum mechanical data (PAPQMD) strategy [31]. Restrained Electrostatic Potential fit change model (RESP) atomic electric charges of the $Ac_3c$ dipeptide were computed at the HF/6-31G(d) level [32]. Finally, parameters for the $\phi$ and $\psi$ torsions were derived by fitting the Ramachandran map of the residue computed at the HF/6-31G(d) level. Starting values of the parameters for angle $\psi$ were derived by fitting the HF/6-31G(d) torsional energy potential of the model molecule cyclopropanecarboxylamide, computed a 15° increments with a truncated Fourier series.

Using the set parameters developed, the adiabatic map of the energy versus both the $\phi$ and $\psi$ angles for $Ac_3c$ was computed with a grid of points at 10° intervals with a dielectric constant of 1. Calculations were carried out by imposing an artificial barrier of 50 kcal on each of the torsions $\phi$ and $\psi$ to force them to keep their corresponding values on the grid. Minimum-energy conformations were subsequently located by complete geometry optimizations of the low-energy structures.

Ab initio computations in the gas phase and aqueous solution were performed using the Gaussian 94 [33] and MonsterGauss [34] computer programs, respectively. MST/AM1 calculations were performed with an adapted version of MOPAC93 revision 2 [35] and force-field calculations were carried out using the AMBER 4.1 program [36].

## 3 Results and discussion

### 3.1 Gas-phase calculations

The Ramachandran plot for the $Ac_3c$ dipeptide computed at the HF/6-31G(d) level is shown in Fig. 1. The energy is expressed in kilocalorie per mole relative to the lowest energy minimum and contours are plotted every kilocalorie per mole. Due to the symmetry of the molecule, the map has a center of symmetry at the point $\phi = 0°$, $\psi = 0°$. This is a well-known feature that differentiates symmetric α,α-disubstituted amino acid residues from L or D amino acids. The HF/6-31G(d) and MP2/6-31G(d) energies for the minima identified are listed in Table 1. Inclusion of correlation corrections to the energy at the MP2 level only introduces minimal quantitative differences in the relative energies of the minima. Similar results are also observed with regard to the overall shape of the map. The energy profiles of two cross sections of the energy surface at $\phi = \pm 90°$ and $\psi = 0°$, computed at MP2/6-31G(d) and HF/6-31G(d) levels, are shown in Fig. 2. The largest relative difference corresponds to the

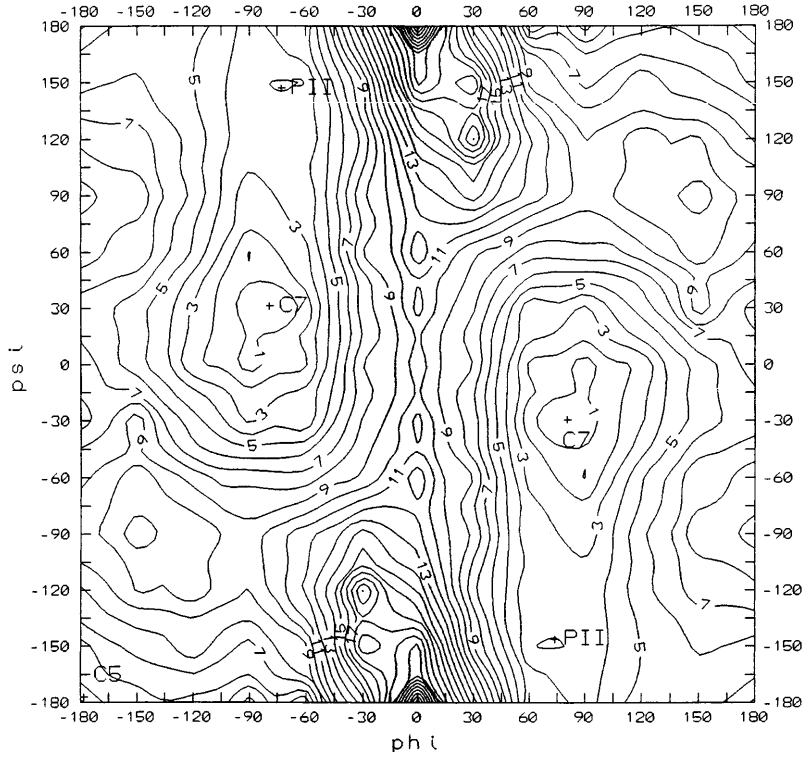


**Fig. 1.** Ramachandran map of the 1-aminocyclopropanecarboxylic acid ($Ac_3c$) dipeptide computed at the Hartree–Fock (*HF*) level with a 6-31(d) basis set. Energies relative to the lowest energy minimum are expressed in kilocalorie per mole. Contours are drawn every kilocalorie per mole. Low energy conformations are explicitly depicted on the map

very compact structure of the (0, 0) point: correlation corrections reduce the height of the central barrier of the Ramachandran plot by almost 2 kcal/mol.

The most striking feature of the $Ac_3c$ dipeptide map is the two symmetric low-energy regions at $\phi$ around $\pm 80°$, which are separated by a high-energy barrier for a value of $\phi = 0°$. These narrow valleys extend over a wide range of $\psi$ values, ranging from $-40$ to $180°$, with the lower areas located at low values of $\psi$. Specifically, the region with $\phi$ around $-80°$ and $\psi$ between 0 and 40° (as well as its respective symmetric region) exhibits energies of 1 kcal/mol above the global minimum that is located on this basin at $\phi = -78.9°$ and $\psi = 31.7°$. This geometry corresponds to a strained $C_7$ conformation that exhibits a hydrogen bond characterized by a O···H bond length of 2.162 Å and a ⟨N—H···O angle of 146.2°.

Two other local minima were characterized: the all-trans $C_5$ conformation ($\phi = 180.0°$, $\psi = 179.9°$) and a polyproline II ($P_{II}$) conformation at $\phi = -71.2°$, $\psi = 145.6°$ that has a symmetrical counterpart. The $C_5$ conformer exhibits an intramolecular interaction between the carbonyl oxygen and the amide hydrogen of the $Ac_3c$ residue, forming a five-membered ring with a H ··· O length of 2.065 Å and a ⟨N—H ··· O angle of 110.4°. It is 3.2 kcal/mol less favored than the global minimum. Both electrostatic and van der Waals interactions contribute to the stability of this conformation, whereas the steric repulsion between the amide groups and the $\beta$ methylene atoms [18] have the opposite effect. Thus, the distances between the $\beta$ methylene hydrogen atoms and the oxygen and hydrogen atoms of the amide groups are 2.50 and 2.20 Å, respectively. The $P_{II}$ conformation corresponds to a shallow minimum. Its relative energy is 2.6 kcal/mol and can be described as an inflexion in the soft slope that goes from $\psi = 90$ to 180° and gets the map from the 3 to 4 kcal/mol level in the bottom of the main valley.

Due to the coarse nature of the grid used to explore the energy surface, other local minima cannot be excluded, but if they exist they must be shallow and would not alter the global shape of the Ramachandran plot. The present results agree with those reported in our previous work [18], where the same three minima were characterized at the HF/6-31G(d) level by geometry optimization of the nine minima that may be anticipated for the potential-energy surface $E = E(\phi, \psi)$. Barone et al. [17] found a minimum 1.8 kcal/mol above the global minimum at $\phi = -88°$, $\psi = -1°$ at the HF/STO-3G level. Similarly, calculations at the HF/3-21G level [18] characterized a minimum 0.3 kcal/mol above the global minimum at $\phi = -95°$, $\psi = 2°$. The present results together with those previously reported [18] confirm that these are spurious minima. However, the Ramachandran plot reveals an ample region at low values of $\psi$ where the molecule can adopt diverse conformations without a large expenditure of energy. In-

**Table 1.** Minimum energy conformations and relative energies for the 1-aminocyclopropanecarboxylic acid ($Ac_3c$) dipeptide. The dihedral angles are in degrees. Minimum energy conformations were characterized at the HF/6-31G(d) level. The relative energies are in units of kilocalorie/mole. Calculations were perfomed on the HF/6-31G(d) minimum energy conformations. Zero-point energies and thermal corrections computed at the HF/6-31G(d) level are included

| No. | $\phi$ | $\psi$ | HF/6-31G(d) | MP2/6-31G(d) |
|---|---|---|---|---|
| $C_7$ | −78.9 | 31.7 | 0.0 | 0.0 |
| $P_{II}$ | −71.2 | 145.6 | 2.6 | 3.7 |
| $C_5$ | 180.0 | 179.9 | 3.2 | 4.6 |

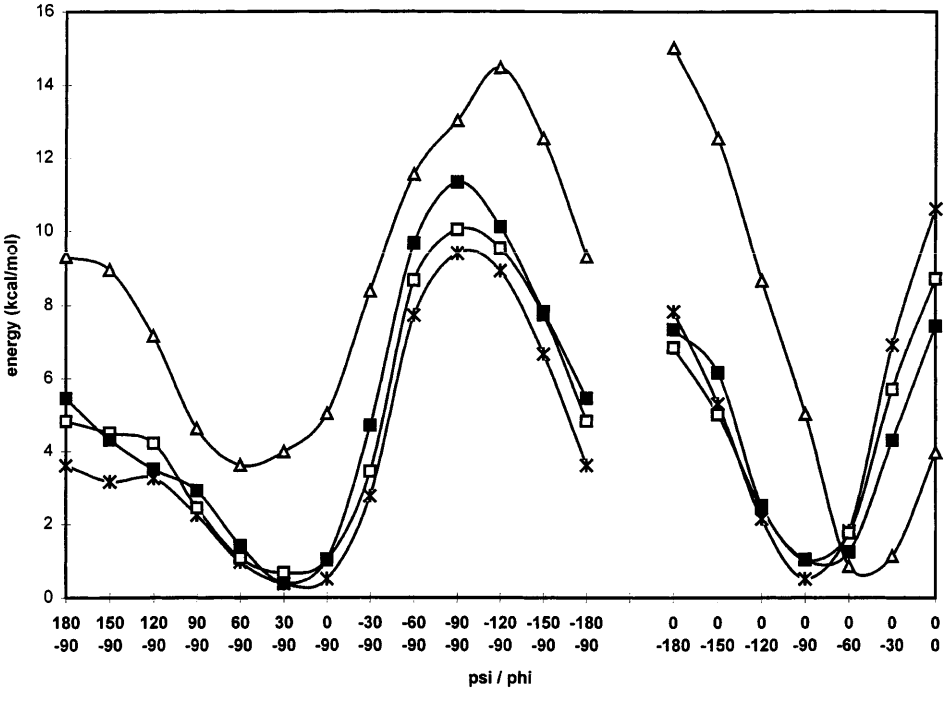


**Fig. 2.** Energies of two cross sections of the Ramachandran map computed at the HF/6-31G(d) (*stars*) and MP2/6-31G(d) (*open squares*) levels, with the AMBER force field using the standard parm94 set of parameters (*open triangles*) and with the AMBER force field using the set of parameters developed in the present work (*filled squares*) levels: **a** energy profile for $\phi = -90°$; **b** energy profile for $\psi = 0°$.

deed, the map reveals that a structure with $\phi = -90°$, $\psi = 0°$ is only 0.52 kcal/mol above the minimum exhibiting a poor hydrogen-bonding interaction: O···H distance of 3.05 Å and a ⟨N—H ··· O angle of 116.8°.

Conformational studies of dipeptide amino acid residues have pointed out the great stability of the $C_7$ conformation in the gas phase. Such stabilization is due to the strong electrostatic effects due to the formation of a hydrogen bond between the carbonyl oxygen in position *i* and the amide proton of the residue i + *3* [20, 21]. Gould et al. [38] studied the alanine and the glycine dipeptides at the HF/6-31G(d,p) level. For the alanine dipeptide the authors found two different $C_7$ minima: $C_{7eq}$ ($\phi = -85.8$, $\psi = 79.0$) and $C_{7ax}$ ($\phi = 76.0$, $\psi = -55.4$) and for the glycine dipeptide a minimum at $\phi = -85.5$, $\psi = 72.0$ and its symmetric counterpart. Similar results were reported for the alanine dipeptide at the MP2/6-31G(d) level [38]. The equilibrium geometry of the $C_7$ conformer of the $Ac_3c$ dipeptide exhibits lower values of $\psi$ than those of glycine or alanine as a consequence of the larger N—$C^{\alpha}$—C angle (119° in comparison to the 115.6° of a standard geometry [39]). This strained geometry provides a weaker hydrogen bond than those found in the alanine and glycine dipeptides. Thus, in order to achieve an effective hydrogen-bonding geometry together with a small value of $\psi$, the $Ac_3c$ dipeptide requires the distortion of the planarity of the $NHCH_3$ amide nitrogen (an improper torsion angle of 153°).

Extended conformation ($C_5$) studies on the alanine and the glycine dipeptides at the HF/6-31G(d,p) level [37, 38] also found a $C_5$ minimum. In the case of the glycine dipeptide, the $C_5$ structure is the global minimum, 0.27 kcal/mol lower than the $C_7$ conformation. For the alanine dipeptide, the $C_5$ conformation is 0.40 kcal/mol above the $C_{7eq}$ structure, but clearly exhibiting lower energy than the $C_{7ax}$ at 2.42 kcal/mol above the global minimum. Again a remarkable difference with the $Ac_3c$ dipeptide appears. Due to the disubstituted character of $Ac_3c$ the comparison uses alanine $C_{7ax}$ as a reference: for the $Ac_3c$ dipeptide the $C_7$ conformer is almost 4 kcal/mol more stable than $C_5$, whereas for the alanine dipeptide the relation is the reverse, $C_5$ being 2.4 kcal/mol more stable than $C_{7ax}$. The MP2 correction of correlation energy changes these figures slightly because of the major corrections in the more compact conformations, but does not affect the general traits.

**Table 2.** Miertus–Scrocco–Tomasi (*MST*)/6-31G(d) free energies of solvation in water ($\Delta G_{sol}$) for the three minima of the $Ac_3c$ dipeptide. Relative values are also displayed. The self-consistent reaction-field (*SCRF*) energy is decomposed into electrostatic ($\Delta G_{pol}$) and steric ($\Delta G_{ster}$) terms. Conformational energies were estimated by adding $\Delta\Delta G_{sol}$ to the gas-phase relative energies computed at the MP2/6-31G(d) level. All values are in kilocalorie per mole

| No. | $\Delta G_{sol}$ | $\Delta G_{pol}$ | $\Delta G_{ster}$ | $\Delta\Delta G_{sol}$ | $\Delta\Delta G_{conf}$ |
|---|---|---|---|---|---|
| $C_7$ | −9.2 | −12.9 | 3.7 | 0.5 | 0.0 |
| $P_{II}$ | −9.7 | −13.4 | 3.7 | 0.0 | 3.2 |
| $C_5$ | −8.3 | −11.8 | 3.5 | 1.4 | 5.5 |

**Table 3.** MST/AM1 free energies of solvation in water ($\Delta G_{sol}$) for the three minima of the $Ac_3c$ dipeptide. Relative values are also displayed. The SCRF energy is decomposed into electrostatic ($\Delta G_{pol}$) and steric ($\Delta G_{ster}$) terms. Conformational energies were estimated by adding $\Delta\Delta G_{sol}$ to the gas-phase relative energies computed at the MP2/6-31G(d) level. All values are in kilocalorie per mole

| No. | $\Delta G_{sol}$ | $\Delta G_{pol}$ | $\Delta G_{ster}$ | $\Delta\Delta G_{sol}$ | $\Delta\Delta G_{conf}$ |
|---|---|---|---|---|---|
| $C_7$ | −9.8 | −13.3 | 3.5 | 0.6 | 0.0 |
| $P_{II}$ | −10.4 | −13.8 | 3.4 | 0.0 | 3.1 |
| $C_5$ | −9.8 | −13.1 | 3.3 | 0.6 | 4.6 |

### *3.2 Aqueous-phase calculations*

Values of $\Delta G_{sol}$ in aqueous solution for the three minimum-energy conformations of the $Ac_3c$ dipeptide at the MST/6-31G(d) and MST/AM1 levels are listed in Tables 2 and 3, respectively. The conformational free-energy difference ($\Delta\Delta G_{conf}$) in solution was estimated by adding $\Delta\Delta G_{sol}$ to the gas-phase relative energy (Eq. 4).

$$\Delta\Delta G_{conf} = \Delta E + \Delta\Delta G_{sol} \quad (5)$$

These results clearly indicate that solute–solvent interactions stabilize the $P_{II}$ conformation with respect to $C_5$ and $C_7$; thus, $P_{II}$ exhibits the most favorable $\Delta G_{sol}$ in aqueous solution at both MST/6-31G(d) and MST/AM1 levels. On the other hand, at the MST/6-31G(d) level the $C_7$ conformation is less stable than the $P_{II}$ one by 0.5 kcal/mol. This result is in good agreement with those provided by the MST/AM1 method, which predicts a destabilization of 0.6 kcal/mol for the $C_7$ conformation. Finally, $\Delta G_{sol}$ of the $C_5$ conformation is 1.4 and 0.6 kcal/mol less favorable than that of $P_{II}$ at the MST/6-31G(d) and MST/AM1 levels, respectively. Thus, comparison of the values displayed in Tables 2 and 3 suggests that solute–solvent electrostatic interactions are slightly overestimated at the MST/AM1 level for the $C_5$ conformation.

An insight into the role of the aqueous solvent on the $Ac_3c$ conformational profile is provided by the $\Delta\Delta G_{conf}$ values reported in Tables 2 and 3. Note that the relative energy order of the low-energy conformations in the gas phase is preserved in aqueous solution, the $C_7$ conformation being the lowest energy conformation in both gas phase and aqueous solution environments. Interestingly, the relative energy of the $P_{II}$ conformation is 0.4–0.5 kcal/mol lower in solution than in the gas phase due to favorable interactions with the solvent. Finally, a $\Delta\Delta G_{conf}$ value of 5.5 and 4.6 kcal/mol is predicted for the $C_5$ conformation at the MST/6-31G(d) and MST/AM1 levels, respectively. Thus, the instability of this conformation in aqueous solution is similar to that predicted in the gas phase calculations.

The different contributions to $\Delta G_{sol}$ are included in Tables 2 and 3. Results indicate that the main difference between the three conformations correspond to the electrostatic contribution, which is larger for $P_{II}$ than for $C_7$ and $C_5$. The differences in the electrostatic contribution for the different conformations are mainly induced by the solvent-exposed surface area of the hydrogen and oxygen atoms of the amide groups, which

are lower in the conformations with intramolecular interactions. Thus, the greater solvent-accessibility of such hydrophilic atoms in the $P_{II}$ conformation increases the favorable electrostatic contribution of $\Delta G_{sol}$ with respect to those of the $C_5$ and $C_7$ conformations.

Due to the good agreement observed between the results provided by the MST/6-31G(d) and MST/AM1 methods, we decided to use the latter to investigate the effect of the aqueous solvent on the whole potential-energy surface of the $Ac_3c$ dipeptide. The $\Delta G_{sol}$ surface obtained at the MST/AM1 level is displayed in Fig. 3. Contour lines are drawn every 0.5 kcal/mol. Comparison of the energy (Fig. 1) and $\Delta G_{sol}$ maps reveals that the solvent tends to stabilize those conformations which are less favorable in the gas phase. The lowest $\Delta G_{sol}$ regions occur for values of $\phi$ around $\pm 90°$ and extend over a range of $\psi$ values from $\pm 80$ to $\pm 40°$. Furthermore, there is another low-energy region located at around $\phi = 0°$ and $\psi = 180°$; however, it should be noted that $\Delta G_{sol}$ increases rapidly, indicating that this is a very narrow region.

Solute–solvent interactions in the low-energy regions found on the gas-phase map at values of $\phi$ around $\pm 80°$ and $\psi$ extending from $\pm 40$ to $180°$ are now less favored than the lowest energy region by at least 4 kcal/mol (Fig. 3). The large differences found between the surfaces displayed in Figs. 1 and 3 can be explained in terms of electrostatic interactions. As first pointed out by Flory [40] in the late 1960s, the alignment of amide bond dipoles is less favored in the gas phase due to repulsive interactions between pairs of atoms with charges of equal sign; however, the large molecular dipole moment obtained from the alignment of the bond dipoles provides more favorable electrostatic interactions with the solvent. Similar trends have also been found in conformational studies of other dipeptides [23, 41, 42].

The $\Delta\Delta G_{conf}$ map for the $Ac_3c$ dipeptide has been computed by adding the gas-phase energies (Fig. 1) and the $\Delta\Delta G_{sol}$ values (Fig. 3) and it is shown in Fig. 4. Interestingly, the map shows only small changes with respect to the gas-phase map. In fact, the only difference between the two maps is a small shift of the lowest energy minimum towards the neighborhood of the point $\phi = \pm 90°$, $\psi = 0°$. These results contrast with the behavior exhibited by other dipeptides. Shang and Head-Gordon [42] studied the effect of introducing the solvent on the ab initio Ramachandran map of the glycine and alanine dipeptides. HF/3-21G surfaces were calculated in vacuo and in a reaction-field representation of water. In those cases the inclusion of the solvent had two major consequences: first, a well-appreciated flattening of the surface, with the subsequent enlargement of the available conformational space; second, the appearance or the deepening of the right- and the left-handed helix minima.

The negligible effect of the aqueous solvent on the conformational preferences of the $Ac_3c$ dipeptide can be understood in terms of the energy map obtained for this residue in the gas phase. Thus, gas-phase energies out of the low-energy regions are very large, i.e. even more than 20 kcal/mol, whereas $\Delta\Delta G_{sol}$ values are much more reduced, i.e. lower than 7 kcal/mol; therefore, the addition of the favorable solute–solvent interactions cannot compensate such unfavorable gas-phase energies. Accordingly, it can be concluded that the intrinsic conformational preferences of this restricted amino acid do not change by introducing environmental factors.

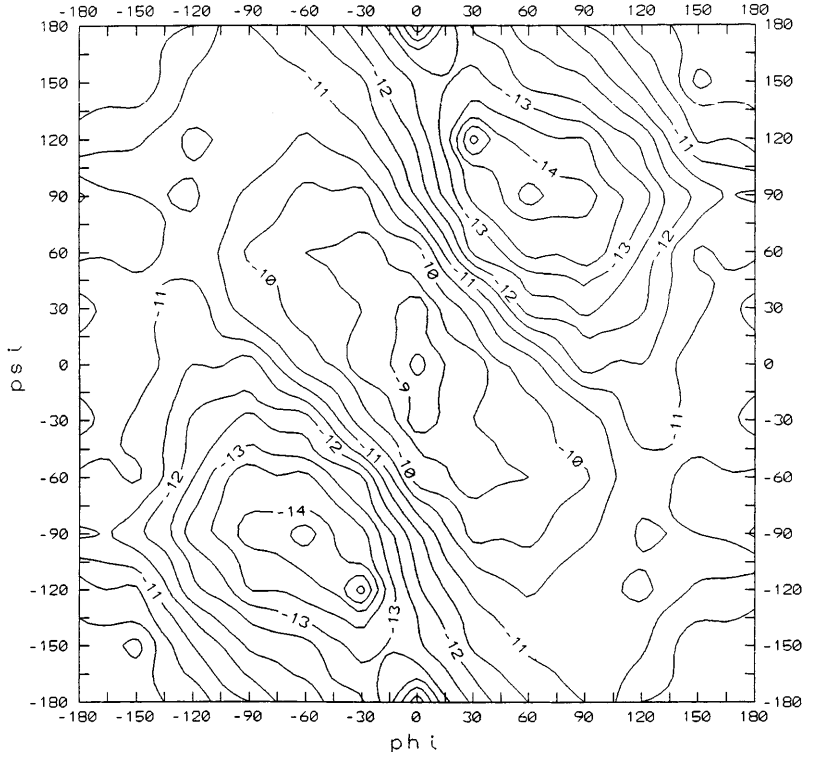


**Fig. 3.** Ramachandran map of the free energy of solvation (in kilocalorie per mole) computed at the Miertus–Scrocco–Tomasi/AM1 level. Contours are drawn every 0.5 kcal/mol

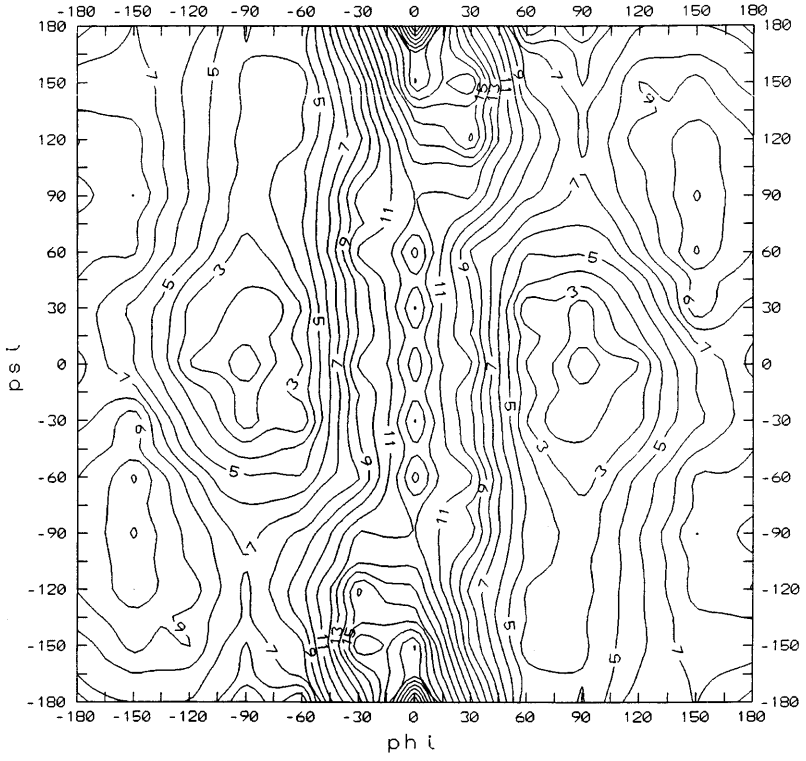


**Fig. 4.** Ramachandran map of the $Ac_3c$ dipeptide computed as the sum of the ab initio gas-phase map and the free energy of solvation map

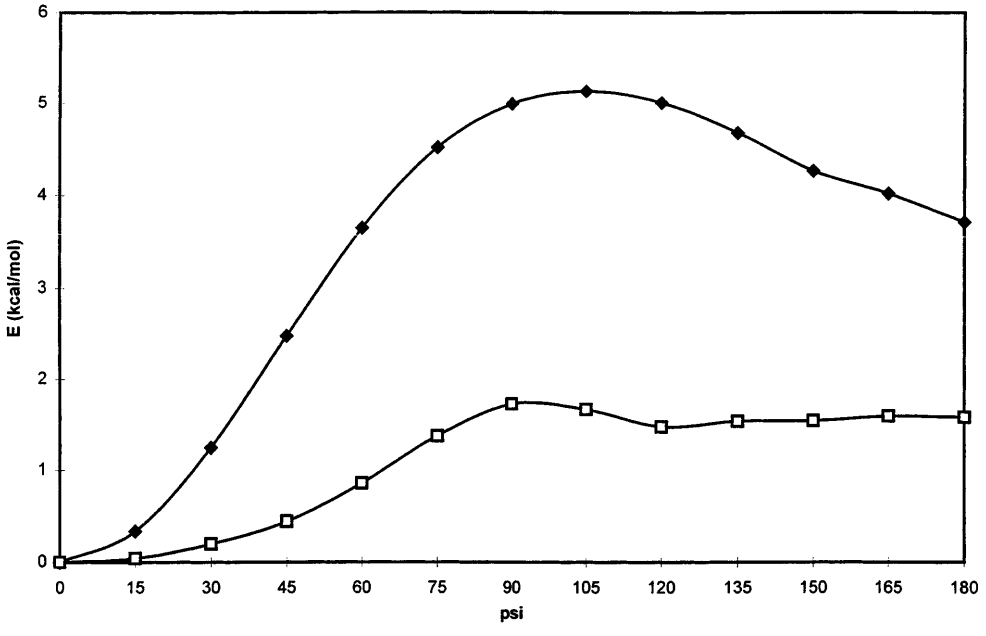


**Fig. 5.** Angle torsional energy profiles of the model molecules cyclopropanecarboxylamide (*filled squares*) and isopropyl-carboxylamide (*open squares*) computed at the HF/6-31G(d) level

### *3.3 Force-field parameterization*

The derivation of bond-stretching and angle-bending parameters was discussed in a previous report [20]. Suffice it to say that these parameters reproduce well the experimentally determined geometries of cyclopropane derivatives with small deviations of 0.007 Å for bond lengths and 1.7° for bond angles. However, it was necessary to introduce new special torsional parameters to reproduce the characteristics of the ab initio potential-energy surface of the $Ac_3c$ dipeptide.

As mentioned in the Methods section, starting values for the torsion of the $\psi$ angle were carried out on the model molecule cyclopropylcarboxamide. The energy profile for the torsion around the C—$C^{\alpha}$—O—N bond for cyclopropylcarboxamide computed at the HF/6-31G(d) level compared with that of isopropylcarboxamide computed at the same level is shown in Fig. 5. For the

former, the transition barrier between the syn and the anti conformations is 5.0 kcal/mol, in good agreement with the experimentally determined value for cyclopropylcarboxaldehyde [16]. In contrast, the barrier for isopropylamide is only 1.7 kcal/mol. However, in both cases the torsional energy profile is asymmetric, with the trans conformer ($\psi = 180°$) being less stable.

The torsional barrier of cyclopropylcarboxamide can be thought to be due to two different contributions:

1. A twofold torsional potential with minima at $\psi = 0°$ and 180°.
2. A stabilization of the former conformer due to steric reasons.

The high energy barrier associated with the twofold torsional potential found in the cyclopropyl model compound can be explained in terms of a hyperconjugative effect [44], due to charge transfer from the oxygen to the carbon for conformations around 90°. In contrast, the lower energy exhibited at $\psi = 180°$ by the isopropyl model compound is of steric origin. Differences between the energy of this conformer for the two model compounds can be explained in terms of a larger steric strain between the amide group and the cyclopropyl hydrogen atoms when compared to the methyl hydrogen atoms of the isopropylcarboxamide. This larger strain originates from the small cyclopropane angle (about 60°) and the very open angle between cyclopropane substituents (about 117°). In contrast, for isopropylcarboxamide the profile is very irregular, suggesting that several factors contribute with a similar weight. The profile in this case can be basically explained by the steric hindrances of the amide group with the two methyl groups, interactions which are absent in the most stable conformation.

The factors discussed for the torsional barrier of cyclopropylcarboxamide account for the special characteristics of the Ramachandran plot of the $Ac_3c$ dipeptide, although there could be masked by the presence of other interactions, and could induce special conformational preferences in peptides containing cyclopropyl-type residues. Torsional barriers have been parameterized using a set of three parameters each associated with a one- two- or threefold rotational barrier. This parameterization fits well the shape of the ab initio energy barrier and provides reasonable barrier heights and angles for the minima located on the force-field surface. Both $\phi$ and $\psi$ torsions were modeled by a combination of three terms: a first-order term of 3.6 kcal/mol, a second-order term 0.50 kcal/mol and a third-order term 0.5 kcal/mol were applied to $\phi$ torsion. Similarly, the torsion around $\psi$ was modeled with a first-order term of 0.4 kcal/mol, a second-order term of 2.5 kcal/mol and a third-order one of 0.90 kcal/mol. The results of this parameterization further support the

**Table 4.** Values of the parameters $V$ and $\gamma$ for the $\phi$ and $\psi$ torsions defined according to the AMBER force field (Ref. 30) developed in the present work

| Torsion | Order | $V$/kcal mol$^{-1}$ | $\gamma$ |
|---|---|---|---|
| $\phi$ | 1 | 0.4 | 180 |
| | 2 | 2.5 | 180 |
| | 3 | 0.9 | 180 |
| $\psi$ | 1 | 0.5 | 0.0 |
| | 2 | 3.6 | 0.0 |
| | 3 | 0.5 | 180 |

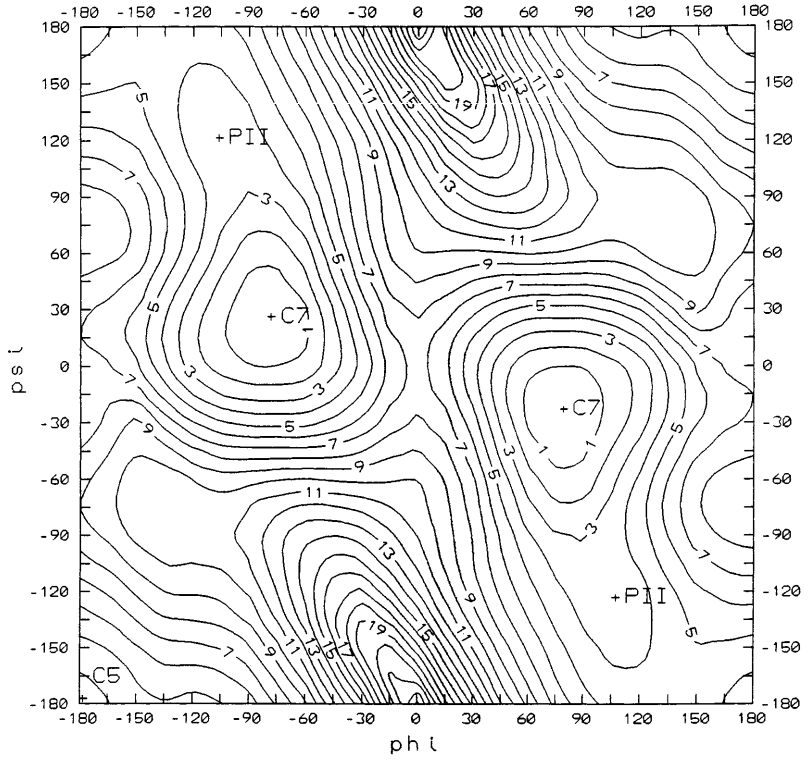


**Fig. 6.** Ramachandran map of the $Ac_3c$ dipeptide computed with the AMBER force field including the new parameters derived in the present work. Low-energy conformations are depicted explicitly on the map

nature of the barrier around $\psi$, since in the Fourier expansion of the torsional potential, first-order terms are associated with dipole-dipole interactions, whereas second-order terms are associated with hyperconjugation [44].

The torsional parameters derived in the present work for the $\phi$ and $\psi$ torsions are listed in Table 4. The rest of the parameters together with the atomic charges for the residue in AMBER format are included in the Appendix. The energy surface obtained with AMBER, after introducing a new set of parameters for the cyclopropane carbons, is shown in Fig. 6. The surface reproduces adequately the features described in the HF/6-31G(d) map. Three energy minima (plus the corresponding ones by symmetry) were located on this surface. The lowest energy minimum is a $C_7$ structure with $\phi = -76°$ and $\psi = 26°$. The second-lowest energy minimum at 3.4 kcal/mol is the $P_{II}$ structure with $\phi = -105°$ and $\psi = 121°$. Finally, the extended conformation, $\phi = -180°$ and $\psi = 180°$, appears at 3.6 kcal/mol. As can be seen, the force-field calculations reproduce with acceptable accuracy the major traits of the HF/6-31G(d) surface, i.e. the location of the absolute minimum and the whole low-energy region, location and relative energy of the other two minima, $C_5$ and $P_{II}$, as well as barrier heights. A quantitative comparison is made in Fig. 2, where the energy profiles of two cross sections of the Ramachandran map are computed at the HF/6-31G(d) and MP2/6-31G(d) levels as well as with the AMBER force field using the parameters developed in the present work.

## 4 Conclusions

The present work reports the results of a conformational study performed on the constrained amino acid residue $Ac_3c$. Ab initio results at the HF/6-31G(d) level indicate the tendency of the residue to adopt conformations with values of $\phi$ around $\pm 80°$ with a wide range of values for $\psi$ from $-40$ to $180°$, with the lower areas located at low values of $\psi$. Three energy minima (and those corresponding by symmetry) were located on the conformational surface. The most stable is the $C_7$ conformation, which is somehow distorted ($\phi = -78$, $\psi = 32$) with regard to the standard conformation ($\phi = -86$, $\psi = 79$), followed by a $P_{II}$ conformation and the extended conformation ($C_5$). MP2 calculations on these structures do not modify the differences in energy between conformations. Solvent effects were also studied using the MST method both at the HF/6-31G(d) level and with the AM1 semiempirical method. The results obtained using these two different levels of calculation are very similar. The free energy of solvation does not modify the conformational features obtained in vacuo, indicating that the tendencies observed are valid in different environments. The most noteworthy effect of the aqueous solvent is a shift of the two absolute minima towards the neighborhood of $\phi = \pm 90°$, $\psi = 0°$, in accord with experimental data and with the known capacity of cyclopropyl amino acids to induce $\beta$-turn conformations in peptides. Finally, ab initio calculations were used to derive new parameters to be able to carry out molecular mechanics calculations with this amino acid residue.

**Appendix**

1-Cyclopropyl AA

| | | | | | | | | | | |
|---|---|---|---|---|---|---|---|---|---|---|
| ACC | INT | 1 | | | | | | | | |
| CORR | OMIT | DU | BEG | | | | | | | |
| 0.00000 | | | | | | | | | | |
| 1 | DUMM | DU | M | 0 | −1 | −2 | 0.000 | 0.000 | 0.000 | 0.00000 |
| 2 | DUMM | DU | M | 1 | 0 | −1 | 1.449 | 0.000 | 0.000 | 0.00000 |
| 3 | DUMM | DU | M | 2 | 1 | 0 | 1.522 | 111.100 | 0.000 | 0.00000 |
| 4 | N | N | M | 3 | 2 | 1 | 1.335 | 116.600 | 180.000 | −0.55700 |
| 5 | HN | H | E | 4 | 3 | 2 | 1.010 | 119.800 | 0.000 | 0.32400 |
| 6 | CA | C4 | M | 4 | 3 | 2 | 1.427 | 121.900 | 180.00 | −0.11600 |
| 7 | CB | C4 | 3 | 6 | 4 | 3 | 1.515 | 118.600 | 300.00 | −0.27300 |
| 8 | H1 | HC | E | 7 | 6 | 4 | 0.996 | 116.400 | −144.500 | 0.09900 |
| 9 | H2 | HC | E | 7 | 6 | 4 | 0.996 | 115.300 | −6.300 | 0.20400 |
| 10 | CC | C4 | B | 7 | 6 | 4 | 1.478 | 61.030 | 106.200 | −0.27300 |
| 11 | H3 | HC | E | 10 | 7 | 6 | 0.996 | 117.900 | 105.600 | 0.09900 |
| 12 | H4 | HC | E | 10 | 7 | 6 | 0.996 | 117.500 | −106.600 | 0.2040 |
| 13 | CO | C | M | 6 | 4 | 3 | 1.500 | 111.100 | 180.000 | 0.88900 |
| 14 | OC | O | E | 13 | 6 | 4 | 1.229 | 120.500 | 0.000 | −0.60000 |

Improper

| | | | |
|---|---|---|---|
| −M | CA | N | HN |
| CA | +M | CO | OC |

Loop

| | |
|---|---|
| CA | CC |

DONE

New parameters for cyclopropyl carbon

| | | | | |
|---|---|---|---|---|
| Mass | | | | |
| C4 | 12.01 | | | |
| Bond | | | | |
| C—C4 317 | | 1.522 | | |
| C4—C4 342 | | 1.501 | | |
| C4—HC 324 | | 1.104 | | |
| C4—N 337 | | 1.435 | | |
| Angle | | | | |
| C4—C—N | 70 | | 116.6 | |
| C4—C—O | 80 | | 120.4 | |
| C—C4—N | 63.0 | | 116.0 | |
| C4—C4—C4 | 232 | | 60.0 | |
| C4—C4—HC | 50 | | 119.1 | |
| C4—C4—N | 80.0 | | 118.7 | |
| HC—C4—HC | 24 | | 111.7 | |
| C—N—C4 | 50 | | 121.9 | |
| C4—N—H | 30 | | 118.4 | |
| C—C4—C4 | 63.0 | | 117.0 | |
| Dihedral | | | | |
| X—C—C4—X | 6 | 0.0 | 0 | 2 |
| X—C4—C4—X | 9 | 1.3 | 0 | 3 |
| X—C4—N—X | 6 | 0.0 | 0 | 3 |
| C4—C4—C—O | 1 | 0.067 | 180 | 3 |
| N—C4—C—O | 1 | 0.067 | 180 | 3 |
| N—C4—C—N | 1 | 0.4 | 180 | −1 |
| N—C4—C—N | 1 | 2.5 | 180 | −2 |
| N—C4—C—N | 1 | 0.90 | 180 | 3 |
| C—N—C4—C | 1 | 0.50 | 0.0 | −2 |
| C—N—C4—C | 1 | 3.6 | 0.0 | −1 |
| C—N—C4—C | 1 | 0.5 | 180.0 | 3 |
| HC—C4—C—O | 1 | 0.067 | 180 | 3 |
| Nonbond | | | | |
| C4 | 1.908 | 0.1094 | | |

END

## References


1. Saragovi HU, Fitzpatrick D, Raktabutr A, Nakanishi H, Kahn M, Greene MI (1991) Science 253: 792
2. Marshall GR (1992) Curr Opin Struct Biol 2: 904
3. Hruby VJ, Kazmierski W, Kawasaki AM, Matsunaga TO (1991) In: Ward DA (ed) Peptide pharmaceuticals. Open University Press, Buckingham, pp 135–184
4. Rizo J, Gierasch LM (1992) Annu Rev Biochem 61: 387
5. Gillespie P, Cicariello J, Olson GL (1997) Biopolymers 43: 191
6. Zimmerman SS, Pottle MS, Nemethy G, Scheraga HA (1977) Macromolecules 10: 1
7. Schimmel PR, Flory PJ (1968) J Mol Biol 34: 105
8. Rose GD, Gierasch LM, Smith JA (1985) Adv Protein Chem 37:1
9. Balaram P (1992) Curr Opin Struct Biol 2: 845
10. Burgess AW (1994) Proc Natl Acad Sci USA 91: 2649
11. Toniolo C (1989) Biopolymers 28: 247
12. Hruby VJ, Al-Obeidi F, Kazmierski W (1990) Biochem J 268: 249
13. Toniolo C, Crisma M, Valle G, Borona GM, Barone V, Benedetti E, Di Blasio B, Pavone V, Pedone C, Santini A, Lelj F (1987) Pept Chem 45
14. Valle G, Crisma M, Toniolo C, Holt EM, Tamura M, Bland J, Stammer CH (1989) Int J Pept Protein Res 34: 56
15. Mapelli C, Newton MG, Ringold CE, Stammer CH (1987) Int J Pept Protein Res 30: 498
16. Volltrauer HN, Schwendeman H (1971) J Chem Phys 54: 260
17. Barone V, Fraternalli F, Cristinziano PL, Lelj F, Rosa A (1988) Biopolymers 27: 1673
18. Aleman C (1997) J Phys Chem 101: 5046
19. Taylor EW, Wilson S, Stammer CH (1991) In: Walters DE, Orthoefer FT, DuBois GE (eds) Sweeteners. Discovery, molecular design and chemoreception. ACS Symposium Series 450. American Chemical Society, Washington, D.C., pp 162–175
20. Aleman C, Casanovas J, Galembeck SE (1998) J Comput Aided Mol Design 12: 259
21. (a) Head-Gordon T, Head-Gordon M, Frisch MJ, Brooks CL III, Pople JA (1991) J Am Chem Soc 113: 5989; (b) Bohm H.J, Brode S (1991) J Am Chem Soc 113: 7129
22. Hu C.H, Shen M, Schaefer HF III (1993) J Am Chem Soc 115: 2913
23. Aleman C, Puiggali J (1997) J Phys Chem B 101: 3441
24. Hariharan PC, Pople JA (1973) Theor Chim Acta 28: 213
25. Miertus S, Scrocco E, Tomasi J (1981) J Chem Phys 55: 117
26. Miertus S, Tomasi J (1982) Chem Phys 65: 239
27. Luque FJ, Bachs M, Orozco M (1994) J Comput Chem 15: 847
28. (a) Bachs M, Luque FJ, Orozco M (1994) J Comput Chem 15: 446; (b) Luque FJ, Negre MJ, Orozco M (1993) J Phys Chem 97: 4386
29. Pierotti RA (1976) Chem Rev 76: 717
30. Cornell WD, Cieplak P, Bayly CL, Gould IR, Merz KM Jr, Ferguson DM, Spellmeyer DC, Fox T, Cadwell JW, Kollman PA (1995) J Am Chem Soc 117: 5179
31. Dewar MJS, Zoebisch EG, Healy EE, Stewart JJP (1985) J Am Chem Soc 107: 3902
32. Aleman C, Canela EI, Franco R, Orozco M (1991) J Comput Chem 12: 664
33. Bayly C, Cieplak P, Cornell W, Kollman PA (1993) J Phys Chem 97: 10269
34. Frisch MJ, Trucks GW, Schlegel HB, Gill PMW, Johnson BG, Robb MA, Cheeseman JR, Keith T, Petersson GA, Montgomery JA, Raghavachari K, Al-Laham MA, Zakrzewski VG, Ortiz JV, Foresman JB, Peng CY, Ayala PY, Chen W, Wong MW, Andres JL, Replogle ES, Gomperts R, Martin RL, Fox J, Binkley JS, Defrees DJ, Baker J, Stewart JJP, Head-Gordon M, Gonzales C, Pople JA (1995) Gaussian 94, revision B.2. Gaussian, Pittsburgh, Pa
35. Cammi R, Bonaccorsi R, Tomasi J (1987) Modified version of Monster Gauss. Peterson M, Poirier R, University of Toronto, Ontario, Canada
36. Stewart JJP (1993) MOPAC93 Revision 2. Fujitsu Limited. Adapted to perform MST calculations by Luque FJ, Orozco M
37. Pearlman DA, Case DA, Cadwell JC, Ross WS, Cheatham TE III, Ferguson DM, Seibel GL, Singh UC, Weiner P, Kollman PA (1995) AMBER4.1. University of California, San Francisco
38. Gould IR, Cornell WD, Hillier IH (1994) J Am Chem Soc 116: 9250
39. Ramachandran GN, Kolaskar AS, Ramakrishnan C, Sasisekharan V (1974) Biochim Biophys Acta 359: 298
40. Flory PJ (1969) Statistical mechanics of chain molecules. Oxford University Press, New York
41. Aleman C, Galembeck SE (1997) J Org Chem 62: 6562
42. Navas JJ, Aleman C, Munoz-Guerra S (1996) J Org Chem 61: 6849
43. Shang HS, Head-Gordon T (1994) J Am Chem Soc 116: 1528
44. Cramer CJ (1996) J Mol Struct (THEOCHEM) 370: 135